Advances in Science and Technology Research Journal

Advances in Science and Technology Research Journal, 18(6), 331–340
https://doi.org/10.12913/22998624/192333
ISSN 2299-8624, License CC-BY 4.0

Received: 2024.06.29
Accepted: 2024.08.15
Published: 2024.09.08

Development and Analysis of Current Collectors for Proton Exchange Membrane Fuel Cells

Aneesh Jose[1,2*], Sudesh Bekal[3], U. Deepika Shanubhogue[4], K. Gurukrishna[4]

[1] Visvesvaraya Technological University, Belgaum, 590018, Karnataka, India
[2] School of Engineering & Technology, Christ University, Bangalore, India
[3] Department of Mechanical Engineering, NMAM Institute of Technology, 574110, Karnataka, India
[4] Department of Physics, Manipal Institute of Technology, Manipal Academy of Higher Education, Manipal 576104, Karnataka, India
* Corresponding author's e-mail: aneeshjones@gmail.com

ABSTRACT

Hydrogen fuel cells are gaining popularity in power-consuming devices due to their zero-emission characteristics. However, ohmic resistance, which arises from the resistance to electron flow through the electrodes and external circuit, can cause reduced efficiency and voltage drops in a fuel cell. This research aims to develop current collector plates for proton exchange membrane fuel cells with optimal design, high electrical conductivity, and thermal conductivity to mitigate ohmic resistance. Six different designs and five different materials-copper, brass, aluminum, stainless steel 316, and stainless steel 304 – were considered for this purpose. The study involved experimental electrical conductivity and fuel cell performance tests to identify the best material and design for the current collector. Results indicated that brass and copper exhibited the least resistivity and favorable material characteristics. Consequently, all six current collector plate designs were developed using brass and copper with various machining and finishing processes. Performance testing on a fuel cell test station revealed that brass current collector plate design 5, featuring open ratios, demonstrated superior performance. Ultimately, the optimum design and material selection of the current collector plates have led to the development of fuel cells with reduced ohmic resistance and improved overall performance.

Keywords: fuel cells, current collectors, bipolar plates, conductivity, thermopower system, resistivity, polarization curves.

INTRODUCTION

A fuel cell is an electrochemical device that converts the chemical energy of a fuel and an oxidizing agent, such as air or oxygen, into electricity through continuous redox reactions. The output of a fuel cell can range from a few milliwatts to several kilowatts. In a proton exchange membrane fuel cell (PEMFC), a Nafion membrane is placed between electrodes coated with a platinum catalyst. The combination of the electrolyte, electrodes, and gas diffusion layer can be assembled to form a membrane exchange assembly (MEA). During the working of the fuel cell, the electrodes release electrons and protons from the fuel. The Nafion membrane allows protons to pass through it while the electrons are forced through an external circuit via MEA, bipolar plate, and current collector plate (CCP). Figure 1 (a) shows an exploded view of the PEMFC. The CCP is placed between the end plates and the bipolar plate on both sides of the MEA. The CCP must effectively contact the bipolar plates to transfer the electrons to the circuit. [1, 2] The current collectors are highly conductive metallic plates in a fuel cell that collect electrons from the bipolar plates and discharge them to an external circuit. The power is then sent to the loading devices or storage, such

as batteries. The current collector may be a mesh plate or a simple structure with protrusions for connecting wires to external connections. [3, 4] Figure 1 (b) provides details of the CCP terminology developed for the in-depth study of the current collector. The CCP is divided into contact and terminal areas. The contact area connects the bipolar plate with the CCP, while the terminal area connects the CCP to an external circuit for electrical transmissions.

A single cell fuel cell produces a voltage of 1 V and the current depends on the surface area of the MEA. Based on the specific design of the fuel cell and fuel cell types, operating conditions influence the power output of the fuel cell. Fuel cell power output can also be expressed in terms of power density which is a measure of watts per square centimeter (W/cm^2), it gives a better expression for the power output capacity of any fuel cell [5, 6, 7].

The overall performance of a fuel cell is reduced by various losses within the fuel cell such as activation, ohmic, and concentration losses. Among these losses, the ohmic loss is due to the flow of electrons in the conductive parts of the fuel cell, and the voltage drop produced by this loss is directly proportional to the current density of the fuel cell. These losses can be expressed by Ohms' law, i.e.

$$\Delta V = I \cdot R_i \tag{1}$$

where: I – current density, A cm^{-2}, and R_i – total cell internal resistance (these include ionic, DC electronic, and contact resistance, Ω cm^2) [8, 9].

$$R_i = R_{ii} + R_{ie} + R_{ic} \tag{2}$$

Fuel cell current collectors should be designed to possess high electric conductivity, low resistance, low ohmic polarization & maximum contact, rugged in nature, and chemical and mechanical stability in the fuel cell working environment. The shape of the current collector should lead to the least contact resistance and withstand the stresses applied on the fuel cell stack at either end of the PEMFC end plates. The current collector should also possess the correct range of surface finish to establish decent contact with the bipolar plate. Current collectors need to transfer the heat produced in the bipolar plates to the cooling mechanisms on the end plates. The quality of the plates' electrical conductivity can be experimentally determined by a four-probe method. A constant direct current (IDC) is applied to the sample through two electrodes. The resulting voltage drop (VΩ) over a portion of the sample with length "t" is measured using one of the two thermocouple wires. Based on the measured voltage drop and the thermocouple distance "t", the specific resistance (ρ) and the electrical conductivity (σ) can be calculated using the following formulas: [10, 11]

$$\rho = (V/I) \times (A/L) \tag{3}$$

where: ρ is the specific resistance, V is the measured voltage drop, I is the impressed current, A is the cross-sectional area of the sample, and L is the length of the sample. The electrical conductivity (σ) can be found as the inverse of the specific resistance:

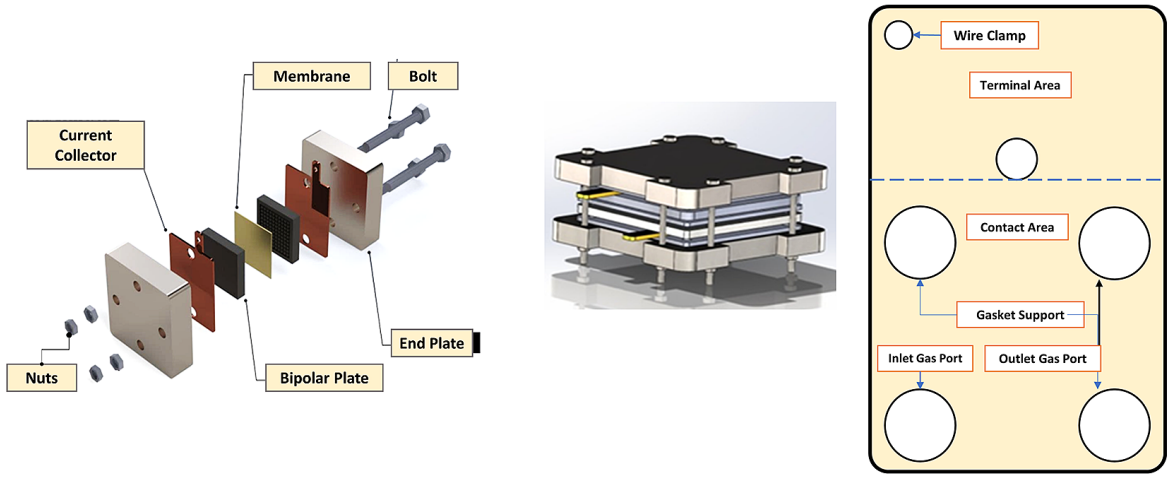

Figure 1. (a) Exploded view of the fuel cell showing the various parts of the fuel cell including the current collector, (b) ISO view of parts of the fuel cell, the golden layer indicates the position of the current collectors which lie between end plates and bipolar plates, (c) details of current collector plate terminology

$$\sigma = 1/\rho \quad (4)$$

From the obtained measurement data, the Seebeck coefficient (S) can then be calculated using the following formula:

$$S = -Vth /(T_{hot} - T_{cold}) \quad (5)$$

where: S is the Seebeck coefficient, Vth is the thermal voltage, T_{hot} is the temperature at the hot junction, T_{cold} is the temperature at the cold junction.

Several researchers have worked with different types of current collectors in PEMFC, a few are summarized here. Braz et. al. studied the current collector with the lower open ratio (34%) on both the anode and cathode sides achieving the best performance with values of 3.14 mW/cm^2 [12]. Peiwen Li in his work reported the decreasing size of the current collector and its control area somewhat improves the power density [13]. Tunahan Gunduz et al. conducted investigations on the effects of current collectors and their geometries in cylindrical fuel cells. The study analyzed pressures, flow rates, and voltages. By using helical flow channels instead of straight ones, the current density increased by approximately 63.18%. [14].

Kuan et al. used a planar graphene thin film current collector for a proton exchange membrane fuel cell (PEMFC). Three different techniques of coatings were used over the fuel cell current collector, it was found that the graphene-dispersed thin film possessed higher surface flatness and long-term studies carried out indicated the higher performance of the fuel cell [15]. The work by Boni M presented research on the influence of the current collector open ratio on a Methanol fuel cell. Experimental results indicated the current collector with a 55.40% open ratio produced the best results [16]. I Zahi et al. in their work on PEMFC carried out CFD modeling to optimize the shape and dimensions of a current collector to identify one with the best electrochemical performance. Three geometries of parallel squares and serpentines were investigated. It has been found that the electrochemical performance was at its best with a trade-off between ohmic losses and overvoltage, also, it was found that the 1 μm thick flat current collector when replaced by an optimal serpentine one, the power density increased by 55% [17]. Fandi Ning et al. in their work on PEMFC using mathematical modeling showed that the performance of any general electrochemical devices can be improved by adjusting the direction of current collectors [18].

RESEARCH METHODOLOGY

This study is unique as it considers electrical aspects, Seebeck effects, and fuel cell performance tests to select the best material, resulting in the development of an efficient CCP for fuel cell applications. The current collector terminology was developed anew for this purpose, as shown in Figure 1c and described above. Six designs were considered, including the conventional design CCD1. The designs were fabricated and developed using five different materials. Stress values and various other properties were compared across different materials. Materials with low resistivity, high yield stress, and low corrosion rates were selected for the design and development of the current collector. Generally, the most commonly used materials for current collectors in fuel cells include graphite, stainless steel, titanium, and copper. Graphite is known for its excellent electrical conductivity and corrosion resistance and is often used in the form of plates or bipolar plates. Stainless steel offers good mechanical strength, electrical conductivity, and corrosion resistance, though it may require coatings to enhance its performance. Titanium provides excellent corrosion resistance and good conductivity; however, it is more expensive compared to other materials. Copper is renowned for its high electrical conductivity but requires protective coatings to prevent corrosion in the fuel cell environment.

In this work, an effort is made to identify economical metals with better conductivity, including aluminum, copper, brass, stainless steel 316, and stainless steel 304. The selected material has been used to develop the current collectors using various machining techniques. Copper has been considered here for comparison with other plate materials. The Current collector plate thickness was restricted to a minimum of 3 mm to withstand a maximum fuel cell tightening torque of 10 Nm, ensuring a proper fit within the fuel cell components. The developed current collectors were subsequently integrated into the fuel cell and evaluated for feasibility, handling, performance, and optimal design. Comparisons were also made against a conventional current collector, used as a standard reference. This standard design is designated as CCD1 (current collector design 1) and was compared with the other five designs.

CURRENT COLLECTOR DESIGNS

The designs of the current collectors considered are based on the dimensions of the bipolar plate assembly and end plates. Figure 2 shows the bipolar plates on the anode and cathode sides respectively. Figure 2a represents the cathode plate, which allows oxygen or oxidants to move from the inlet to the outlet through different channels. Figure 2b is the anode plate that enables hydrogen to pass through it across the channel length. Figure 2c shows the dimensions of the anode plate and the channel widths. The thickness of the plate has been limited to a minimum of 3 mm to provide sufficient strength to withstand the fuel cell tightening torque of up to 10 Nm and suit the screw length. Figure 3 provides details of the six different current collector designs considered in this work.

The design only has open areas at the contact points where the inlet and outlet gas fit into the

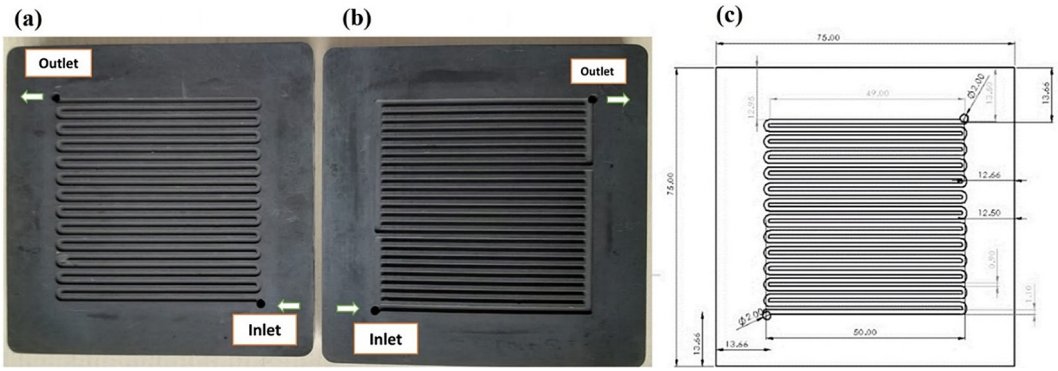

Figure 2. Fuel cell bipolar plates. (a) anode plate (b) cathode plate and (c) design drawing of the plate

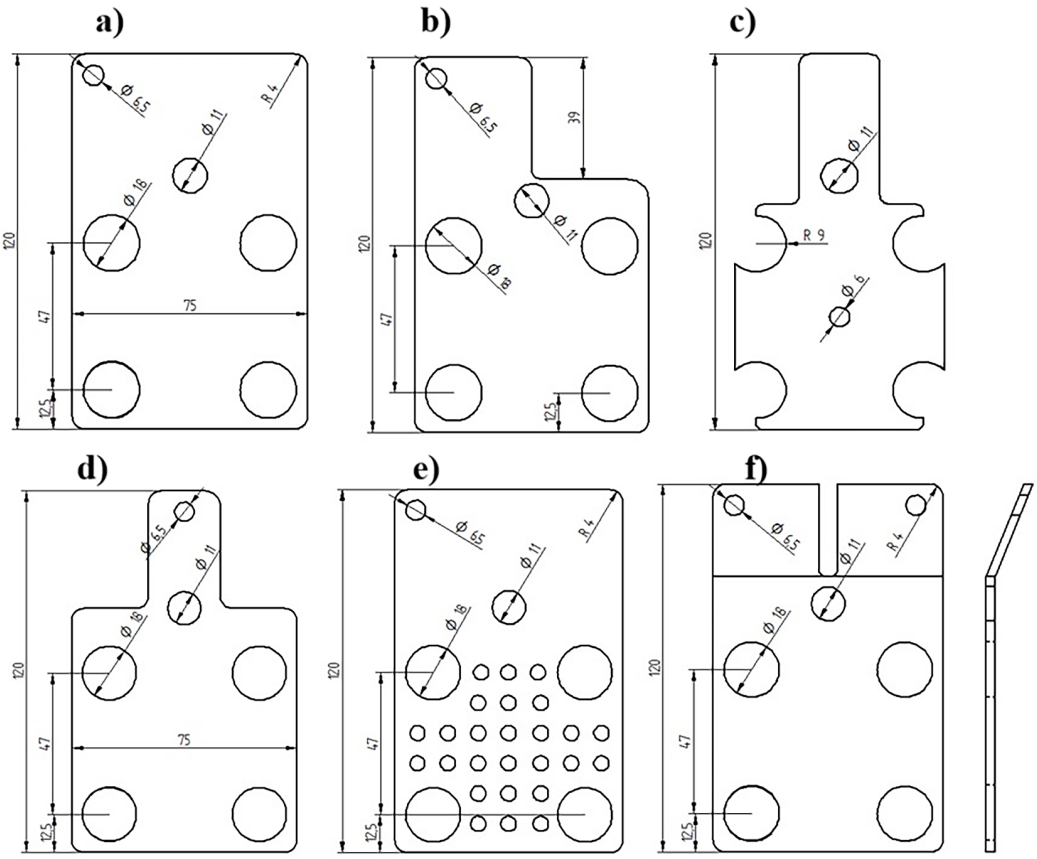

Figure 3. Current collector plate designs; (a) CCD1; current collector design 1, (b) CCD2; current collector design 2, (c) CCD3; current collector design 3, (d) CCD4; current collector design 4, (e) CCD6; current collector design 5, (f) CCD6; current collector design 6 – front and side view (all dimensions in mm)

bipolar plate. CCD2 is similar to CCD1, except the terminal section has been cut in half, making it easier to access and view the bipolar plates from the top. There will also be space between the current collector plates on either side. CCD3 has contact only at the center of the bipolar plate and does not cross outside the port areas. This design reduces the overall contact surface and has the least contact and terminal areas. CCD4 has a protrusion at the center and material removed from the sides. The bipolar plates can be accessed from either side of the current collector plate, but there is a disadvantage of terminal wire accumulation at the center and low strength at the terminal area. CCD5 has open holes, which increases the open ratio and improves the overall conductivity of the plate. CCD6 has terminal sections that are bent at an angle of 20 degrees from the axis of the plate, and the terminal section is cut into thin slices at the center. This design helps when the number of terminal wires is numerous and additional equipment such as temperature probes need to be fixed on the fuel cell. Table 1 provides the design details and dimensions of all six current collector designs taken into consideration.

EXPERIMENTAL DETAILS

Experiments are carried out to find resistivity and Seebeck effects for all five materials chosen. The material is chosen based on high electric conductivity, good surface finish, rugged nature, and mechanical stability in the fuel cell working environment. The five materials considered here are copper, Brass, Aluminum, Stainless steel 316, and Stainless steel 304. The specimens of each material have been developed for the same. The second set of experiments is carried out to find the performance of fuel cells with different designs and materials of the CCP, for this purpose CCP's of all six designs and materials have been developed with various machining techniques.

Experimental resistivity/Seebeck coefficient analysis

Resistivity tests were carried out on samples of the current collector for five different materials on an LSR-3 High-Temperature thermopower Resistivity on the LINSEIS Platform. The experimental four-point probe system consists of four electrodes organized in an intermediate linear array as shown in Figure 4a and b. Seebeck coefficients and resistivity have been found for increasing temperatures and graphs are plotted. Figure 4a is the experimental apparatus, and Figure 4b is the four probes making contact with the specimen, two at the center and one ether at the upper and lower ends. Figure 4c gives the details of the specimen dimension maintained for the test purpose. Seebeck coefficient character is inversely proportional to carrier concentration and also the electrical conductivity, therefore can be used in conductivity assessment [19].

FUEL CELL PERFORMANCE

Experiments are conducted to identify the performance of the fuel cell with different designs of the CCPs. The fuel cells are set up with each design of the developed CCPs and their performance polarization is plotted. The flow of oxygen and hydrogen is varied between 0.1 and 0.2 liters/minute, and the circuit pressure of the hydrogen line is set between 2 bar to 3 bar for the oxygen pressure line. The fuel cell is loaded from 0.1 amps to a maximum of 10 amps, with steps of 0.5 – ampere current values, while the variation of voltage and current is noted down. All experiments are conducted within the range of 60–80 °C. Figure 5 (a) shows the fuel cell with a CCD2 design made with a brass collector being tested on the fuel cell test station. Figure 5 (b) is the flow diagram of the computerized fuel cell test station.

Table 1. Comparison of all six designs of the current collector

S. no	CC design	Area (mm^2)	Open ratio (%)	Terminal area (mm^2)	Contact area (mm^2)	No of open holes
1.	CCD1	7858	12.67	3622	4232	6
2.	CCD2	6392	15.19	1875	4232	6
3.	CCD3	5750	3.5	1500	3815	2
4.	CCD4	5865	16.3	1633	4232	6
5.	CCD5	7344	18.5	3622	3722	32
6.	CCD6	7641	13.3	3409	4232	7

Figure 4. (a) Schematic of LINSEIS standard LSR-3 measurement system and (b) LSR-3 System probes connected to the specimen. (c) Test Specimens and their dimensions for testing conductivity on LSR-3

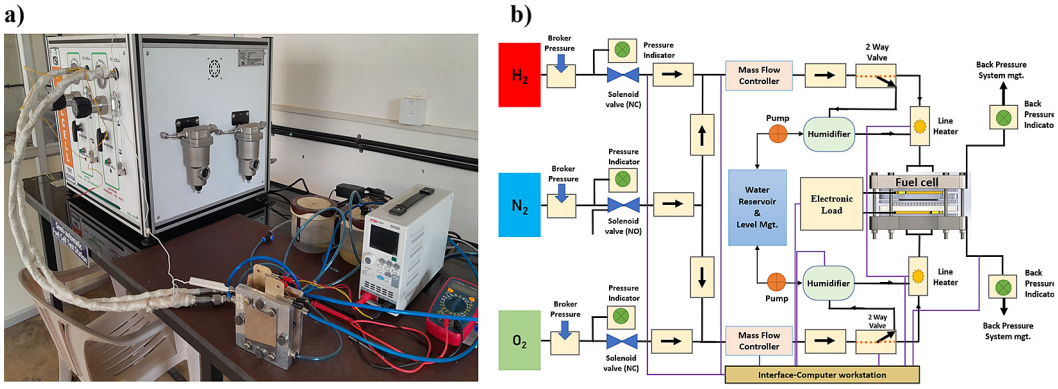

Figure 5. (a) Fuel cell work station with a PEM fuel cell and brass current collector plate (CCD2 design) and (b) fuel cell work station flow diagram

Figure 6 displays the six different designs of the plates and their assembly in the fuel cell. All current collectors, except CCD3, were developed using simple drilling and cutting processes based on the dimensions in Figure 3. CCD3 was manufactured using a wire EDM (electric discharge machine), which resulted in the best finishing among all other methods. The surface roughness was measured with a handysurf surface roughness tester, and surface grinders and sand sheets were used for fine finishing to ensure uniformity across all collectors. Figure 6 (a) to Figure 6 (g) illustrates all six developed current collectors and their placements in the fuel cell.

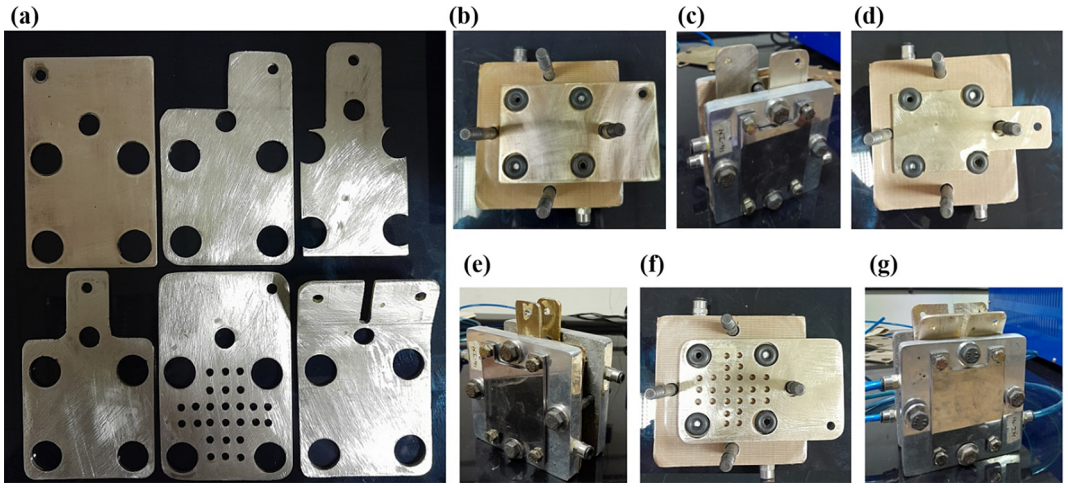

Figure 6. (a) Developed Brass plate current collectors – all six designs (CCD1-CCD6) and (b) CCD1 (c) CCD2 (d) CCD3 (e) CCD4 (f) CCD5 and (g) CCD6, current collector assembly on the fuel cell for all six plates

RESULTS AND DISCUSSIONS

Material assortment

Figure 7 gives the plots of resistivity experimentally determined by the four-probe method. All the materials have been analyzed for their resistivity at varying temperatures of 40 °C to 140 °C, this is the working temperature of PEMFC and the resistivity is measured at intervals of 10 °C. Figure 7b gives the resistivity vs. temperature plot for five different material specimens taken from CCPs. From the plot aluminum, copper and brass show the least resistivity in the range of 0–0.1 µOhm·m. Stainless steel 316 and 304 showed elevated resistivity in the range of 0.6–0.7 µOhm·m.

Figure 7a, 7b illustrates the Seebeck effect and resistivity for the five materials tested, while Figure 7b presents the resistivity versus temperature plot for five different material specimens taken from Current Collector Plates (CCPs). The materials analyzed in this study include copper, brass, stainless steel 316, and stainless steel 304. Copper is considered the standard material due to its high thermal and electrical conductivity and is most commonly used for high-conductivity applications. Figure 7a illustrates the Seebeck effect for the five materials tested. The data indicates that brass exhibits the highest Seebeck coefficient, followed by aluminum and copper. The Seebeck coefficient hierarchy is Al < Cu < Brass < SS316 < SS304. Conversely, the resistivity rankings are Brass < Al < Cu < SS304 < SS316. These findings suggest that brass, copper, and aluminum are viable candidates for current collector plates from resistivity and Seebeck coefficient perspectives. In contrast, stainless steels (SS316 and SS304) are unsuitable for current collector plates due to their higher resistivity values.

Current collectors on the fuel cells are subjected to compressive forces at the collector area and bending stress on the terminal area as they are sandwiched between bipolar and end plates and fastened by nuts and bolts. On average 50W single-plate fuel cell parts are fastened

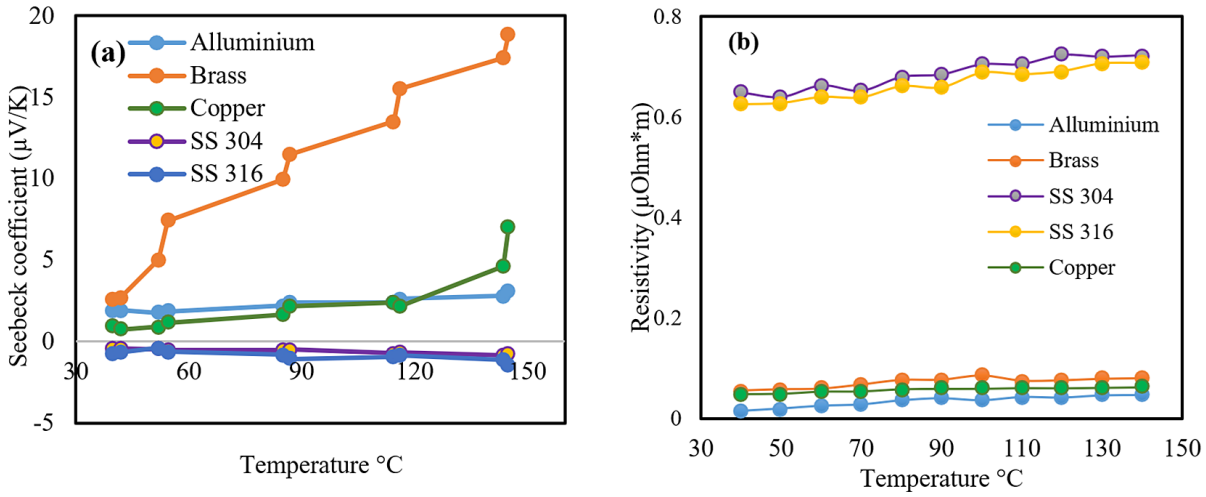

Figure 7. Experimental results of temperature vs. resistivity for five different materials. (a) seebeck coefficient vs. temperature and (b) resistivity vs temperature graphs for five materials

Table 2. Material properties for a 3mm thick current collector

S. no	Material	Yield strength (MPa)	Hardness rockwell (B-Scale)	Density (Kg/m³)	CTE, linear 250 °C µm/m- °C	Thermal conductivity Wm−1 K−1	Resistivity (µOhm·m)
1.	Copper	33.3	51	8850	16.4	385	0.0584
2.	Brass	130	65	8730	18.5	110	0.0767
3.	Al	125	60	2680	21	237	0.0361
4.	SS 304	215	70	8000	17.8	15	0.6799
5.	SS 316	220	88	8000	16.5	14	0.6614

with a torque of 5–10 Nm. They are also subjected to temperature stresses during chemical reactions which may cause them to expand. The current collector plates have been assessed for their thermal conductivity since they need to be agents of heat transfer from bipolar plates to end plates. The materials considered for the current collector have also been analyzed for the stresses it can handle. Stress, hardness, and density values are taken from the literature and other experimentally determined values are listed in Table 2 [20, 21, 22].

Table 2 displays the different properties of the five materials considered, steel has the highest yield strength and hardness, however, copper and brass have higher density. The yield strength helps the current collector to withstand the forces acting on it and to hold the connections on the terminal areas. However, steels have high resistivity and lower thermal conductivity issues. From the conductivity analysis, brass, aluminum, and copper showed better results. Aluminum was found to have the least resistivity and best conductivity. Brass and copper have close values of resistivity; however, brass has a higher strength value, higher Seebeck coefficients, and better corrosion resistance compared to that of copper and aluminum. Copper has high corrosion affinity and tarnishing issues, least Rockwell hardness number compared to Brass and aluminum. Brass also can withstand the tightening pressures of the end plates due to higher yield stress, hence brass has been considered as the ideal material for the current collectors.

Design assortment

The initial set of experiments focused only on the CCD1 current collector design, and five different materials were tested for comparison purposes. This set of experiments aimed to identify variations in the performance of the current collector for a single design by changing the materials used. In the second set of experiments, brass materials were used for all six different designs (CCD1-CCD6) tested. The second set of experiments focused on evaluating the performance of a Proton Exchange Membrane (PEM) fuel cell. These tests were conducted using a fuel cell test station. Since PEM fuel cells typically – of the current collector were carried out within this specific range. [23, 24] The aim was to assess how different current collector designs influence the overall performance of the fuel cell under typical operating conditions. [25, 26, 27] Figure 8a and Figure 8b illustrate the fuel cell performance using six different designs of current collectors, with experiments conducted on a Fuel Cell Test Station. In these figures, Current Collector Design 1 (CCD1) serves as the standard reference for comparison with the other current collector designs.

In Figure 8a, the variations in fuel cell performance are minimal when using different materials for the current collector with the standard CCD1 design. However, Figure 8b shows that significant changes in the polarization curve occur as the design of the current collector is altered. These observations highlight the impact of

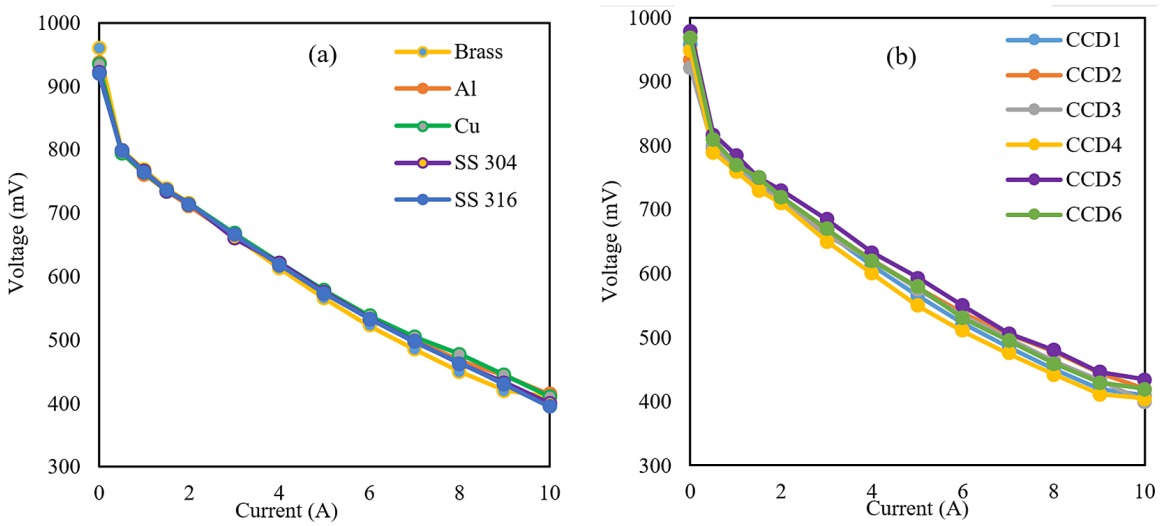

Figure 8. (a) Current vs. voltage chart for different materials of CCD1. (b) current vs. voltage plot for all six designs (CCD1-CCD6)

both material selection and design configuration on the overall performance of the fuel cell. As depicted in Figure 8a, the maximum voltage of 980 mV is observed in the activation region (0–2 Amps), while it drops to a minimum in the concentration regions (8́–10 Amps) a common trend in fuel cells attributed to polarization losses. Notably, the brass plate current collector achieves the highest voltage in the activation region. The descending order of voltage performance among the materials is as follows: Brass, copper (Cu), aluminum (Al), stainless steel 304 (SS304), and stainless steel 316 (SS316).

The polarization curve graphs reveal only slight variations, but it is noteworthy that the CCD6 current collector outperforms others across all three regions of the I-V graph, as shown in Figure 8b. It delivers approximately 3% better performance in all regions, including the ohmic region at 2–8 Amperes. The performance order from highest to lowest is as follows: CCD5, CCD6, CCD2, CCD1, CCD3, and CCD4. The open ratios in CCD5 contribute to improved contact, reduced contact resistance, and increased stress concentration areas, leading to lower resistivity and enhanced conductivity. Conversely, the CCD4 design shows poor performance due to its small contact area, which was included to achieve a distinctive design.

CONCLUSIONS

The study intended to develop metallic current collector plates (CCPs) for PEM fuel cells, evaluating five different materials and six distinct designs. Resistivity tests conducted using the LSR-3 high-temperature thermopower resistivity measurement on the LINSEIS platform revealed that brass, copper, and aluminum exhibited the lowest resistivity values, ranging from 0 to 0.1 μOhm-m. In contrast, steel demonstrated higher resistivity (0.6–0.7 μOhm-m) and was consequently deemed unsuitable as a CCP material due to its poor conductivity. Notably, brass showed a 10% higher Seebeck coefficient than aluminum. Based on these findings, six CCP designs were developed using brass and copper. Fuel cell performance tests were subsequently conducted to evaluate these designs. The CCD5 design, featuring an open ratio, enhanced fuel cell performance by 3% compared to the simpler CCD2 design, with CCD6 following closely at a 1.5% improvement. These results suggest reduced ohmic losses in the more advanced designs. Moreover, the CCD6 and CCD5 designs proved superior in managing fuel cell operations and terminal area connections. Future research could focus on examining the effects of corrosion and the integration of various base materials with protective coatings on CCP performance, providing further insights into optimizing fuel cell efficiency.

Acknowledgement

This work was supported by All India Council for Technical Education (AICTE) grant funded by the Government of India (No.8-168/FDC/RPS(Rural)/POLICY-1/2021-22) and NMAM Institute of Technology (NITTE-deemed to be university). The authors thank profusely for the support provided by the two organizations.

REFERENCES

1. Fan L.F.L., Tu Z., Chan S.H. Recent development of hydrogen and fuel cell technologies: A review, Energy Reports, 2021; 7: 8421–8446, https://doi.org/10.1016/j.egyr.2021.08.003
2. Shaoxuan Z., Weijian Y., Xiaoqiang L., Jiamu C., Front Y.Z. Output power regulation system for portable micro fuel cell systems, Frontiers in Energy Research, 2023; 11. https://doi.org/10.3389/fenrg.2023.1118743
3. Adamson K.A., Butler J., Hugh M. Fuel cell today industry review: Fuel cells: Commercialization Platinum Met. 2008; 52(2): 123. https://doi.org/10.1595/147106708X292508
4. Jiao, K., Xuan, J., Du, Q., Bao, Z., Xie, B., Wang, B., Zhao, Y., Fan, L., Wang, H., Hou, Z., Huo, S., Brandon, N.P., Yin, Y., Guiver, M.D. Designing the next generation of proton-exchange membrane fuel cells. Nature 2021; 595: 361–369. https://doi.org/10.1038/s41586-021-03482-7
5. Wang, Y., Chen, K.S., Mishler, J., Cho, S.C., Adroher, X.C. A review of polymer electrolyte membrane fuel cells: Technology, applications, and needs on fundamental research. Applied Energy, 2011; 88(4): 981–1007. https://doi.org/10.1016/j.apenergy.2010.09.030
6. Performance characterization of high surface area Pt/C cathode catalyst layers in PEM fuel cells" by Celik, I., Matian, M., Smirnova, A.L., Electrochimica Acta, 2020, https://doi.org/10.1016/j.electacta.2020.136093

7. Su Y., Yin C., Hua S., Wang R., Tang H. Study of cell voltage uniformity of proton exchange membrane fuel cell stack with an optimized artificial neural network model, International Journal of Hydrogen Energy, 2022; 47: 67, https://doi.org/10.1016/j.ijhydene.2022.06.240
8. Jordy S., Mayken E.-A., Tingshuai L., Andersson M. A detailed analysis of internal resistance of a PEFC comparing high and low humidification of the reactant gases. Frontiers in Energy Research, 2020. https://doi.org/10.3389/fenrg.2020.00217
9. Zhang X., Zhao Y., Xu L., Hu Z., Zhao G., Sun H., Li J. and Ouyang M. Polarization decomposing of proton exchange membrane fuel cell considering liquid water accumulation. Journal of The Electrochemical Society, 2022; 169: 124517. https://doi.org/10.1149/1945-7111/aca6a8
10. Salhani C., Rastikian J., Barraud C., Lafarge P., Della Rocca M.L. Seebeck coefficient of thin films close to the metal-insulator transition for molecular junctions. Physical Review Applied, 2019; 11(1): 014050. https://doi.org/10.1103/PhysRevApplied.11.014050
11. Gomi H., Yoshino T. Resistivity, seebeck coefficient, and thermal conductivity of platinum at high pressure and temperature. Physical Review B, 2019; 100(21): 214302. https://doi.org/10.1103/PhysRevB.100.214302
12. Braz B.A., Moreira C.S., Oliveira V.B., Pinto A.M.F.R. Effect of the current collector design on the performance of a passive direct methanol fuel cell. Electrochimica Acta, 2019. https://doi.org/10.1016/j.electacta.2019.01.131
13. Li P., Ki J.P., Liu H. Analysis and optimization of current collecting systems in PEM fuel cells. International Journal of Energy and Environmental Engineering 2012; 1–10. https://doi.org/10.1186/2251-6832-3-2
14. Gunduz T., Demircan T. Numerical analysis of the effects of current collector plate geometry on performance in a cylindrical PEM fuel cell, International Journal of Hydrogen Energy, 2022; 47(39): 17393–17406. https://doi.org/10.1016/j.ijhydene.2022.03.221
15. Yean-Der K., Ke T.-R., Lyu J.-L., Sung M.-F., and Do J.-S. Development of a current collector with a graphene thin film for a proton exchange membrane fuel cell module. Molecules 2020; 4: 955. https://doi.org/10.3390/molecules25040955
16. Boni, M., Surapaneni, S.R., Golagani, N.S. Experimental investigations on the effect of current collector open ratio on the performance of a passive direct methanol fuel cell with liquid electrolyte layer. Chem. Pap 2021; 75: 27–38. https://doi.org/10.1007/s11696-020-01277-0
17. Rossi Z.C., Faucheux V. Micro PEM fuel cell current collector design and optimization with CFD 3D modeling. International Journal of Hydrogen Energy, 2011. https://doi.org/10.1016/j.ijhydene.2011.08.020
18. Ning, F., Shen, Y., Bai, C., Wei, J., Lu, G., Cui, Y., Zhou, X. Critical importance of current collector property to the performance of flexible electrochemical power sources. Chinese Chemical Letters 2019. https://doi.org/10.1016/j.cclet.2019.02.032
19. Sun H., Zhang G., Guo L.-J. A novel technique for measuring current distributions in PEM fuel cells, Journal of Power Sources 2006; 158(1): 326–332. https://doi.org/10.1016/j.jpowsour.2005.09.046
20. Pukha V.E., Glukhov A.A., Belmesov A.A., Kabachkov E.N., Khodos I.I., Khadem M., Kim D.-E., Karaseov P.A. Corrosion-resistant nanostructured carbon-based coatings for applications in fuel cells based on bipolar plates, Vacuum 2023. https://doi.org/10.1016/j.vacuum.2023.112643
21. Asri N.F., Husaini T., Sulong A.B. Coating of stainless steel and titanium bipolar plates for anticorrosion in PEMFC: A review, International Journal of Hydrogen Energy 2017; 42(14): 9135–9148. https://doi.org/10.1016/j.ijhydene.2016.06.241
22. Shi J., Zhang P., Han Y., Wang H., Wang X., Yu Y., Sun J. Investigation on electrochemical behavior and surface conductivity of titanium carbide modified Ti bipolar plate of PEMFC, International Journal of Hydrogen Energy 2020; 45(16): 10050–10058. https://doi.org/10.1016/j.ijhydene.2020.01.203
23. Che J., Yi P., Peng L., Lai X. Impact of pressure on carbon films by PECVD toward high deposition rates and high stability as metallic bipolar plate for PEMFCs, International Journal of Hydrogen Energy 2020; 45(32): 16277–16286. https://doi.org/10.1016/j.ijhydene.2020.04.078
24. Sahu I.P., Krishna G., Biswas M., Das M.K. Performance study of PEM fuel cell under different loading conditions. *Energy Procedia,* 2014; *54*: 468–478. https://doi.org/10.1016/j.egypro.2014.07.289
25. Addala S., Naidu I.E.S. Modeling and analysis of fuel cell power generation system using proportional integral speed controller. Adv. Sci. Technol. Res. J. 2024; 18(2): 187–195. https://doi.org/10.12913/22998624/184340
26. Addala S., Naidu I.E.S. Investigation of sodium hydroxide on the electrolysis and silica based nano fluid on the performance of proton exchange membrane fuel cell. Adv. Sci. Technol. Res. J. 2024; 18(5): 413–420. https://doi.org/10.12913/22998624/191313
27. Marappan, M., Palaniswamy, K., Velumani, T., Chul, K.B., Velayutham, R., Shivakumar, P., Sundaram, S. Performance studies of proton exchange membrane fuel cells with different flow field designs – Review, 2021. The Chemical Record. https://doi.org/10.1002/tcr.202000138